A New Random Walk Model for PCS Networks

Ian F. Akyildiz, *Fellow, IEEE*, Yi-Bing Lin, *Senior Member, IEEE*, Wei-Ru Lai, and Rong-Jaye Chen

***Abstract*—This paper proposes a new approach to simplify the two-dimensional random walk models capturing the movement of mobile users in Personal Communications Services (PCS) networks. Analytical models are proposed for the new random walks. For a PCS network with hexagonal configuration, our approach reduces the states of the two-dimensional random walk from $(3n^2 + 3n - 5)$ to $n(n+1)/2$, where n is the layers of a cluster. For a mesh configuration, our approach reduces the states from $(2n^2 - 2n + 1)$ to $(n^2 + 2n + 4)/4$ if n is even and to $(n^2 + 2n + 5)/4$ if n is odd. Simulation experiments are conducted to validate the analytical models. The results indicate that the errors between the analytical and simulation models are within 1%. Three applications (i.e., microcell/macrocell configuration, distance-based location update, and GPRS mobility management for data routing) are used to show how our new model can be used to investigate the performance of PCS networks.**

***Index Terms*—Cell, mobility management, personal communications services, random walk.**

I. Introduction

In *Personal Communications Services* (PCS) systems, the service areas are covered by radio base stations (BS's) [12]. The radio coverage of a BS is called a *cell*. A mobile phone or mobile station (MS) moves from one cell to another. Most PCS performance studies assume that the cells are configured as a hexagonal network given in Fig. 1 or a mesh network given in Fig. 2. To investigate the MS movements is a challenging problem in PCS. For example, starting from a particular cell, the destination cell of an MS after k movements is determined in [2]. Another example is given in [15], which studied how many steps an MS should make to leave a region.

A two-dimensional random walk model with absorbing states [9] can be used to study the movements of an MS. In this model, a state represents a cell where the MS may reside. Fig. 1 shows a 6-subarea hexagonal cluster. The cell at the center of the cluster is called *subarea-0* cell. The cells surrounding the subarea $(x-1)$ cells are called *subarea* x cells. There are $6x$ cells in subarea x except that exactly one cell is in subarea 0. An n-subarea cluster contains cells from subarea 0 to subarea $(n-1)$. The cells surrounding the subarea $(n-1)$ cells are referred to as *boundary neighbors*, which are outside of the cluster. Fig. 2 shows a 5-subarea mesh cluster. In this network, every cell has four neighbors and an MS can only move to one of the four neighboring cells.

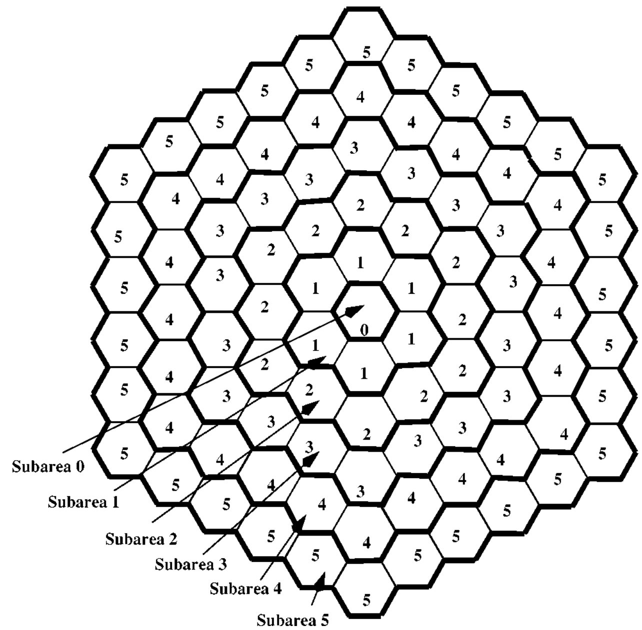

Fig. 1. Hexagonal PCS cell structure.

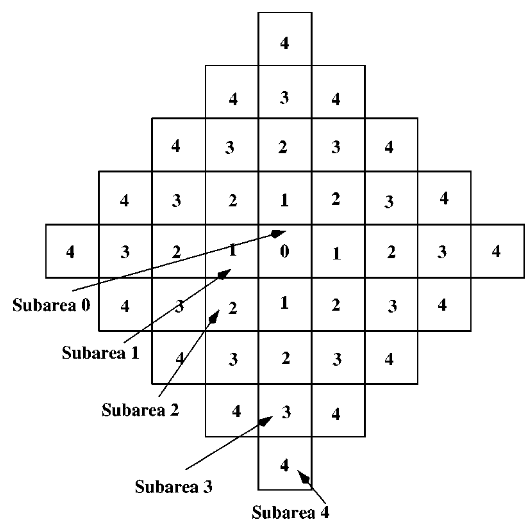

Fig. 2. Mesh PCS cell structure.

To compute the number of movements, whenever an MS moves out of the region, i.e., moving to a boundary cell, the random walk enters an *absorbing* state. A potential problem of this model is that the number of states increases rapidly as the size of the region increases. To reduce the computational complexity, we modified the two-dimensional random walk model

Manuscript received October 6, 1999; revised February 23, 2000. The work of I. F. Akyildiz was supported by the National Science Foundation (NSF) under Grant NCR-97-04393.

I. F. Akyildiz is with Broadband and Wireless Networking Lab., School of Electrical and Computer Engineering, Georgia Institute of Technology, Atlanta, GA 30332 USA (e-mail: Ian.Akyildiz@ee.gatech.edu).

Y.-B. Lin and R.-J. Chen are with the Department of Computer Science and Information Engineering, National Chiao Tung University, Hsinchu, Taiwan, R.O.C. (e-mail: liny@csie.nctu.edu.tw; rjchen@csie.nctu.edu.tw).

W.-R. Lai is with the Department of Information Management, Chin-Min College, Tou-Fen, Miao-Li, Taiwan, R.O.C. (e-mail: wrlai@mis.chinmin.edu.tw).

Publisher Item Identifier S 0733-8716(00)05415-9.

TABLE I
THE ACRONYM LIST

BS: Base Station
BTS: Base Transceiver Station
GPRS: General Packet Radio Service
GSM: Global System for Mobile Communication
GTP: GPRS Tunneling Protocol
MS: Mobile Station
LA: Location Area
PCS: Personal Communications Services
RA: Routing Area

given in [2]. However, the modified model has been simplified, which introduces some inaccuracy to the two-dimensional random walk models.

In this paper, we show how to reduce the two-dimensional random walks for hexagonal and mesh planes such that the simplified random walks behave exactly the same as the original random walks. The paper is organized as follows. Section II describes the new random walk for hexagonal configuration. Section III shows how to group cells with the same routing patterns so that the states in the random walk can be reduced. Section IV validates our model with simulation experiments. Section V elaborates on how to use a similar technique to reduce the states for a mesh random walk model. Section VI illustrates three applications that benefit from our random walk model. The acronyms used in the paper are listed in Table I.

II. The Two-Dimensional Hexagonal Random Walk

Let us consider a hexagonal plane. We assume that an MS resides in a cell for a period, then moves to one of its neighbors with the same probability, i.e., with probability 1/6; see Fig. 3. We derive the number k of moving steps (a step represents an MS movement from a cell to another) from the starting cell until the MS moves out of the cluster.

Based on the assumption that the routing probabilities are equal, we observe that the cells in a cluster can be classified into several types, where a type represents a state in the new random walk. The term "type" is defined as follows.

Definition 1: Two cells A and B are of the same type if the multiset of types for A's neighbors is the same as that for B's neighbors.

A multiset is a collection of objects that are not necessarily distinct. The multiplicity of elements has significance in the type definition.

The 6-subarea cluster is shown in Fig. 4 where lines 1–3 divide the cluster into 6 equal pieces. Exchange of any two pieces has no impact on the structure of the cluster. If two cells, for example, the cells marked with •, are at the same relative position on different pieces, then they are grouped together and assigned to the same type. MS's in the cells of the same type will leave the cells with the same routing pattern. It is intuitive that cells in different subareas should have different types. In the next section, we describe a type classification algorithm based on the 3-line symmetry concept, which satisfies Definition 1.

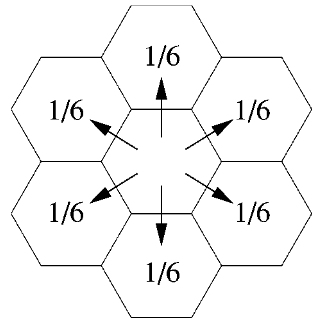

Fig. 3. The hexagonal routing pattern.

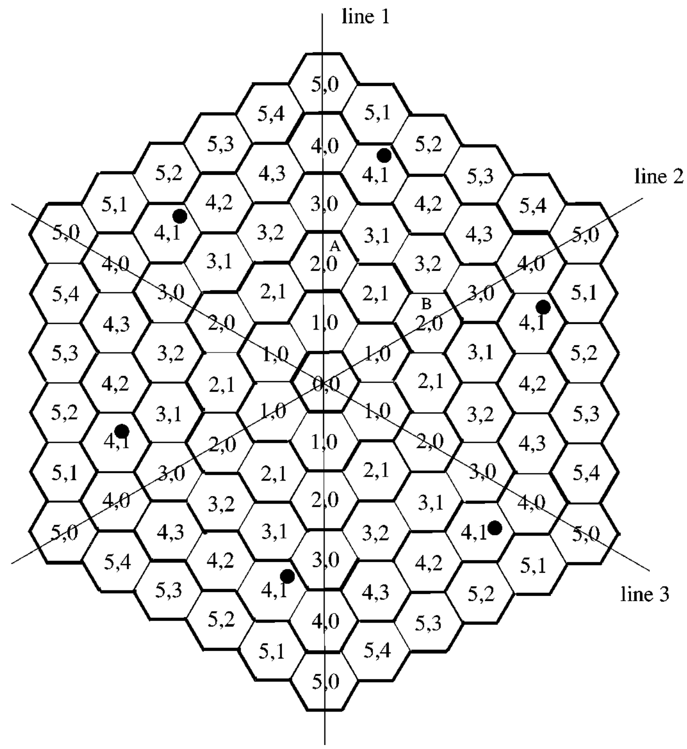

Fig. 4. The type classification in a 6-subarea cluster.

III. The Type Classification for Hexagonal Random Walk

Here we describe a type classification algorithm which satisfies Definition 1. This algorithm recursively assigns types for cells in an n-subarea cluster. Basically, every cell is marked as type $\langle x, y \rangle$, where "x" represents that the cell is in subarea-x, and "y" $\geq$ 0 represents the $y+1$st type in subarea-x. The algorithm is described as follows.

The Type Classification Algorithm for an N-Subarea Cluster:

Step 1) The subarea-0 cell is assigned to type $\langle 0, 0 \rangle$. $x \leftarrow 0$ (x is the subarea of cells being labeled).

Step 2) $x \leftarrow x + 1$. If $x = n$, then Stop.

Step 3) Find unmarked subarea-x cells that have one $\langle x - 1, 0 \rangle$ neighboring cell. Label them by type $\langle x, 0 \rangle$. $y \leftarrow 0$ (y represents the $y+1$st type in subarea-x).

Step 4) Let $y \leftarrow y + 1$. If $y = x$, then go to Step 2.

Step 5) Find unmarked subarea-x cells that are the neighbors of $\langle x, y-1\rangle$ cells in the clockwise direction. Mark them with type $\langle x, y\rangle$. Go to Step 4.

It is easy to verify that the classification algorithm has the following three properties:

1) For $n > 1$, the $\langle 0, 0\rangle$ cell has six $\langle 1, 0\rangle$ neighboring cells. For $n = 1$, it has six $\langle 0, 0\rangle$ boundary neighbors.
2) For a $\langle x, 0\rangle$ cell (where $1 \le x < n-1$), the multiset of types of its six neighboring cells is $\{\langle x-1, 0\rangle, \langle x, x-1\rangle, \langle x, 1 \bmod x\rangle, \langle x+1, 0\rangle, \langle x+1, 1\rangle, \langle x+1, x\rangle\}$. For $x = n-1$, the multiset of $\langle x, 0\rangle$ is $\{\langle x-1, 0\rangle, \langle x, 1 \bmod x\rangle, \langle x, x-1\rangle$, boundary $\langle x, 0\rangle$, boundary $\langle x, 0\rangle$, boundary $\langle x, 1 \bmod x\rangle\}$, where "boundary $\langle x, y\rangle$" represents the type of the boundary neighbor out of the cluster.
3) For a $\langle x, y\rangle$ cell (where $0 \le y \le x-1$), if $x < n-1$, the multiset of types of its six neighboring cells is $\{\langle x-1, y-1\rangle, \langle x-1, y \bmod (x-1)\rangle, \langle x, y-1\rangle, \langle x, (y+1) \bmod x\rangle, \langle x+1, y\rangle, \langle x+1, y+1\rangle\}$. For $x = n-1$, the multiset of $\langle x, y\rangle$ is $\{\langle x-1, y-1\rangle, \langle x-1, y \bmod (x-1)\rangle, \langle x, y-1\rangle, \langle x, y+1 \bmod x\rangle$, boundary $\langle x, x-y\rangle$, boundary $\langle x, x-y+1 \bmod x\rangle\}$.

The above properties ensure that the classification algorithm satisfies Definition 1.

Fig. 4 illustrates the types of cells for a 6-subarea cluster classified by the algorithm. Cells are assigned to types $\langle x, y\rangle$, where "x" indicates that the cell is in subarea-x, and $y \ge 0$ represents the $y+1$st type in subarea-x. The cell in subarea-0 is of the type $\langle 0, 0\rangle$. The six subareas-1 cells are of the same type $\langle 1, 0\rangle$ because they have the same neighboring types (i.e., one $\langle 0, 0\rangle$, two $\langle 1, 0\rangle$ cells and three boundary neighbors). For a 2-subarea cluster, a subarea-2 cell may have 2 or 3 boundary neighbors and is assigned to type $\langle 2, 1\rangle$ or $\langle 2, 0\rangle$, respectively. By following the same method, we mark all cells subarea by subarea. It is easy to verify that the resulting type assignment satisfies Definition 1. For example, consider cells A and B in Fig. 4. These cells are assigned to type $\langle 2, 0\rangle$. Both multisets of types for A's and B's neighbors are $\{\langle 1, 0\rangle, \langle 3, 0\rangle, \langle 3, 1\rangle, \langle 3, 2\rangle, \langle 2, 1\rangle, \langle 2, 1\rangle\}$. Thus, A and B are grouped together and are assigned to type $\langle 2, 0\rangle$.

Based on the type classification and the concept of absorbing states, the state diagram of the random walk for an n-subarea cluster (where $n = 6$) is shown in Fig. 5. In this state diagram, state (x, y) represents that the MS is in one of the cells of type $\langle x, y\rangle$, where $0 \le x < n$ and $0 \le y \le x-1$. State (n, j) represents that the MS moves out of the cluster from state $(n-1, j)$, where $0 \le j < n-1$. For $0 \le x < n$ and $0 \le y \le x-1$, states (x, y) are transient and for $0 \le j < n-1$, states (n, j) are absorbing.

Let $p_{(x,y),(x',y')}$ be the one-step transition probability from state (x, y) to state (x', y'); i.e., the probability that the MS moves from a $\langle x, y\rangle$ cell to a $\langle x', y'\rangle$ cell in one step. Since all neighbors of the $\langle 0, 0\rangle$ cell are $\langle 1, 0\rangle$ cells, the process moves from state (0, 0) to state (1, 0) with probability $p_{(0,0),(1,0)} = 1$. A $\langle 1, 0\rangle$ cell has one $\langle 0, 0\rangle$ neighbor, and the transition from state (1, 0) to state (0, 0) has probability $p_{(1,0),(0,0)} = 1/6$. The transition back to a state itself occurs when the MS moves to a cell of the same type. Since each $\langle 1, 0\rangle$ cell has two $\langle 1, 0\rangle$ neighbors, state (1,0) has a transition back to itself with probability $p_{(1,0),(1,0)} = 1/3$. For $0 \le j < n-1$, $p_{(n-1,j),(n,j)}$ is the probability that the MS moves from a $\langle n-1, j\rangle$ cell to a neighbor out of the cluster in one step. The absorbing state (n, j) loops back to itself with probability $p_{(n,j),(n,j)} = 1$, for $0 \le j < n-1$.

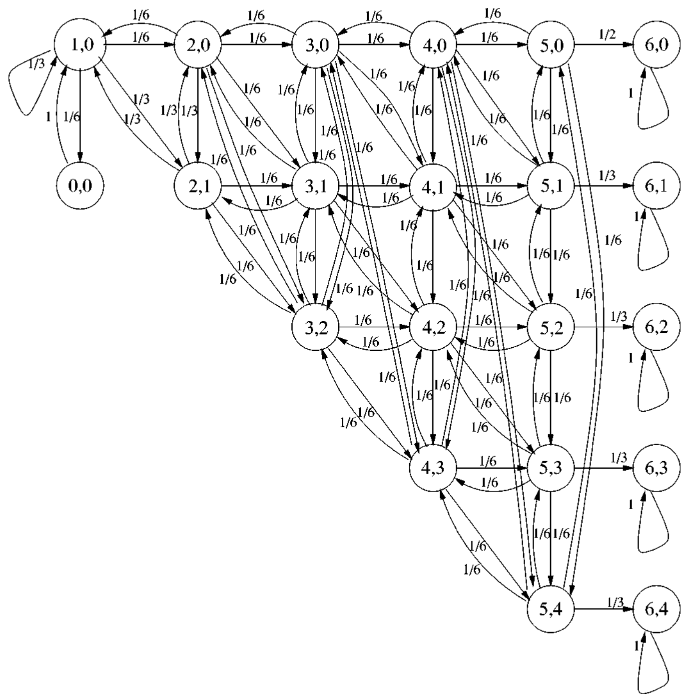

Fig. 5. State diagram for a 6-subarea cluster.

Let $S(n)$ be the total number of states for an n-subarea cluster random walk. Then $S(1) = 2$ and if $n > 1$

$$S(n) = \frac{n(n+1)}{2}.$$

The *transition matrix* of this random walk is an $S(n) \times S(n)$ matrix $\boldsymbol{P} = (p_{(x,y),(x',y')})$ where

$$\boldsymbol{P} = \begin{pmatrix} 0 & 1 & 0 & 0 & 0 & \cdots & 0 & 0 & 0 \\ 1/6 & 1/3 & 1/6 & 1/3 & 0 & \cdots & 0 & 0 & 0 \\ 0 & 1/6 & 0 & 1/3 & 1/6 & \cdots & 0 & 0 & 0 \\ 0 & 1/3 & 1/3 & 0 & 0 & \cdots & 0 & 0 & 0 \\ \vdots & \vdots & \vdots & \vdots & \vdots & \ddots & \vdots & \vdots & \vdots \\ 0 & 0 & 0 & 0 & 0 & \cdots & 1 & 0 & 0 \\ 0 & 0 & 0 & 0 & 0 & \cdots & 0 & 1 & 0 \\ 0 & 0 & 0 & 0 & 0 & \cdots & 0 & 0 & 1 \end{pmatrix}_{S(n)\times S(n)}.$$

For $n = 6$, $S(n) = 21$, and in this matrix, the elements in each column and row are listed in the following (x, y) order: (0, 0), (1, 0), (2, 0), (2, 1), (3, 0), (3, 1), $\cdots$, (6, 3), and (6, 4). We use the Chapman–Kolmogorov equation [18] to compute the probability for the number of steps that an MS moves from a cell type to another. For $k \ge 1$, let

$$\boldsymbol{P}^{(k)} = \begin{cases} \boldsymbol{P}, & \text{if } k = 1 \\ \boldsymbol{P} \times \boldsymbol{P}^{(k-1)}, & \text{if } k > 1. \end{cases} \tag{1}$$

An element $p^{(k)}_{(x,y),(x',y')}$ in $\boldsymbol{P}^{(k)}$ is the probability that the random walk moves from state (x, y) to state (x', y') with exact k steps. For $0 \le j < n-1$, define $p_{k,(x,y),(n,j)}$ as

$$p_{k,(x,y),(n,j)} = \begin{cases} p_{(x,y),(n,j)}, & \text{for } k = 1 \\ p^{(k)}_{(x,y),(n,j)} - p^{(k-1)}_{(x,y),(n,j)}, & \text{for } k > 1. \end{cases} \tag{2}$$

Then $p_{k,(x,y),(n,j)}$ is the probability that an MS initially resides at a $\langle x, y\rangle$ cell, moves into a $\langle n-1, j\rangle$ cell at the $k-1$st step, and then moves out of the cluster at the kth step. Our new hexagonal random walk model reduces the states from $(3n^2 + 3n - 5)$ to $n(n+1)/2$. In the next section, we validate the new random walk by simulation experiments.

IV. Performance Comparisons

Suppose that an MS initially resides at a $\langle x, y\rangle$ cell. Then the expected number of steps that the MS stays in a 6-subarea cluster is computed as

$$K_{\langle x,y\rangle} = \sum_{k=1}^{\infty} \sum_{j=0}^{4} k \cdot p_{k,(x,y),(6,j)}. \tag{3}$$

Equation (3) is validated by simulation experiments following the procedure described in [19]. In the ith simulation experiment, we simulate the movement of an MS in a 6-cluster to compute the number $\tilde{k}_{\langle x,y\rangle}(i)$ of steps that the MS moves from a $\langle x, y\rangle$ cell to a boundary cell (outside the cluster). Let $\tilde{K}_{\langle x,y\rangle}$ be the $K_{\langle x,y\rangle}$ value obtained from M_1 simulation experiments, where

$$\tilde{K}_{\langle x,y\rangle} = \frac{1}{M_1} \sum_{i=1}^{M_1} \tilde{k}_{\langle x,y\rangle}(i). \tag{4}$$

We calculate $\tilde{K}_{\langle x,y\rangle}$ with $M_1 = 1\,200\,000$ simulation experiments and use 200 truncated terms in $K_{\langle x,y\rangle}$ to approximate the infinite summations. Table II shows the results from (3) and (4). The discrepancy between (3) and (4) is within 0.3% for all test cases.

The expected number of steps that the MS leaves the cluster through a $\langle 5, z\rangle$ cell is computed as

$$L_{\langle 5,z\rangle} = \sum_{k=1}^{\infty} \sum_{x=0}^{5} \sum_{y=0}^{x-1} k \cdot p_{k,(x,y),(6,z)}. \tag{5}$$

Equation (5)is also validated by simulation experiments. From the simulation experiments, we compute $\tilde{L}_{\langle 5,z\rangle}$ using an equation similar to (4). Table III shows the results derived from analytic computations and simulation experiments. The discrepancy between them is within 1% for all test cases.

V. Two-Dimensional Mesh Random Walk

The two-dimensional mesh random walk model can be simplified following the same concept described in the previous sections. The routing pattern for a mesh cell is shown in Fig. 6. We assume that an MS resides in a cell for a period, then moves to one of its neighbors with the same probability, i.e., with probability 1/4.

TABLE II
Comparison of $K_{\langle x,y\rangle}$ (Analysis) and $\tilde{K}_{\langle x,y\rangle}$ (Simulation) for 6-Cluster Hexagonal Configuration

(x,y)	$(0,0)$	$(1,0)$	$(2,0)$	$(2,1)$
$K_{\langle x,y\rangle}$	29.157	28.158	25.167	26.156
$\tilde{K}_{\langle x,y\rangle}$	29.08	28.090	25.130	26.104
Error	0.26%	0.24%	0.15%	0.20%
(x,y)	$(3,0)$	$(3,1)$	$(3,2)$	$(4,0)$
$K_{\langle x,y\rangle}$	20.249	22.144	22.144	13.658
$\tilde{K}_{\langle x,y\rangle}$	20.224	22.099	22.101	13.627
Error	0.12%	0.20%	0.19%	0.23%
(x,y)	$(4,1)$	$(4,2)$	$(4,3)$	$(5,0)$
$K_{\langle x,y\rangle}$	16.191	16.961	16.191	6.139
$\tilde{K}_{\langle x,y\rangle}$	16.173	16.911	16.186	6.142
Error	0.11%	0.29%	0.03%	−0.05%
(x,y)	$(5,1)$	$(5,2)$	$(5,3)$	$(5,4)$
$K_{\langle x,y\rangle}$	8.589	9.548	9.548	8.589
$\tilde{K}_{\langle x,y\rangle}$	8.577	9.540	9.526	8.583
Error	0.14%	0.08%	0.23%	0.07%

TABLE III
Comaprison of $L_{\langle x,y\rangle}$ (Analysis) and $\tilde{L}_{\langle x,y\rangle}$ (Simulation) for 6-Cluster Hexagonal Configuration

(x,y)	$(5,0)$	$(5,1)$	$(5,2)$	$(5,3)$	$(5,4)$
$L_{\langle x,y\rangle}$	52.014	52.5664	60.7217	60.7217	52.5664
$\tilde{L}_{\langle x,y\rangle}$	51.5089	52.4964	60.8102	60.8025	52.4644
Error	0.97%	0.13%	−0.15%	−0.13%	0.19%

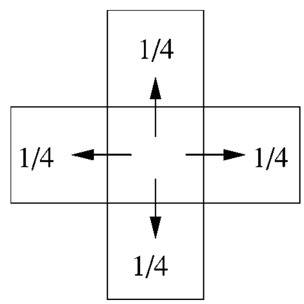

Fig. 6. The mesh routing pattern.

Fig. 7 illustrates the types of cells. Following a type assignment procedure similar to the one described in the previous section, cells are assigned to types $\langle x, y\rangle$, where x indicates that the cell is in subarea-x, and $y \ge 0$ represents the $y+1$st type in subarea-x.

Based on the type classification and the concept of absorbing states, the state diagram of a 4-subarea mesh random walk is shown in Fig. 8. In this state diagram, state (x, y) represents that the MS is in one of the cells of type $\langle x, y\rangle$. State (4, 0) is an absorbing state and represents that the MS moves out of the cluster.

Let $p_{(x,y),(x',y')}$ be the one-step transition probability from state (x, y) to state (x', y'); i.e., the probability that the MS moves from a $\langle x, y\rangle$ cell to a $\langle x', y'\rangle$ cell in one step. Then the

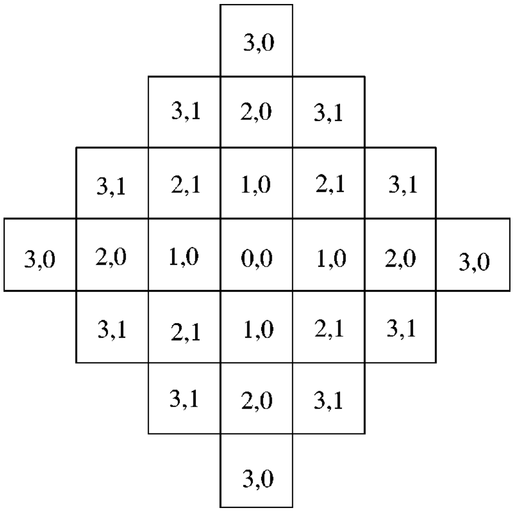

Fig. 7. Type classification for a 4-subarea mesh cluster.

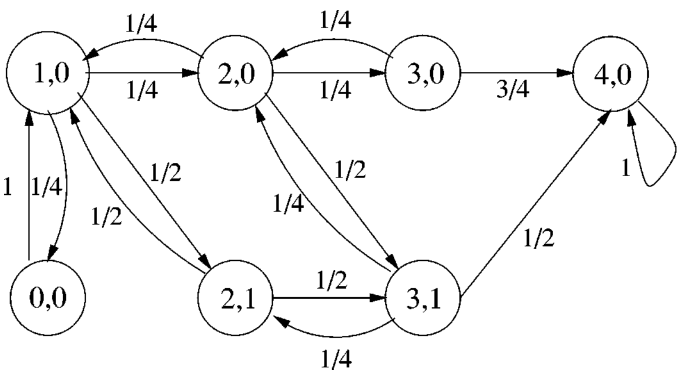

Fig. 8. State diagram for a 4-subarea mesh cluster.

transition matrix of the 3-subarea random walk is a 7×7 matrix $\boldsymbol{P} = (p_{(x,y),(x',y')})$ where

$$\boldsymbol{P} = \begin{pmatrix} 0 & 1 & 0 & 0 & 0 & 0 & 0 \\ 1/4 & 0 & 1/4 & 1/2 & 0 & 0 & 0 \\ 0 & 1/4 & 0 & 0 & 1/4 & 1/2 & 0 \\ 0 & 1/2 & 0 & 0 & 0 & 1/2 & 0 \\ 0 & 0 & 1/4 & 0 & 0 & 0 & 3/4 \\ 0 & 0 & 1/4 & 1/4 & 0 & 0 & 1/2 \\ 0 & 0 & 0 & 0 & 0 & 0 & 1 \end{pmatrix}_{7\times 7}.$$

In this matrix, the elements in each column and row are listed in the following (x, y) order: (0, 0), (1, 0), (2, 0), (2, 1), (3, 0), (3, 1), and (4, 0). It is clear that our new mesh random walk model reduces the states from $(2n^2 - 2n + 1)$ to $(n^2 + 2n + 4)/4$ if n is even and to $(n^2 + 2n + 5)/4$ if n is odd. Following (1) and (2), we compute $p_{k,(x,y),(4,0)}$. The state diagram in Fig. 8 is validated by simulation experiments by comparing the $K_{\langle x,y\rangle}$ and $\tilde{K}_{\langle x,y\rangle}$ values defined in (3) and (4). Table IV shows that the discrepancy between $K_{\langle x,y\rangle}$ and $\tilde{K}_{\langle x,y\rangle}$ is within 0.2% for all test cases.

TABLE IV
COMPARISON OF $K_{\langle x,y\rangle}$ (ANALYSIS) AND $\tilde{K}_{\langle x,y\rangle}$ (SIMULATION) FOR 4-CLUSTER MESH CONFIGURATION

(x,y)	(0,0)	(1,0)	(2,0)
$K_{\langle x,y\rangle}$	9.681	8.681	5.983
$\tilde{K}_{\langle x,y\rangle}$	9.674	8.688	5.995
Error	0.04%	0.01%	−0.08%
(x,y)	(2,1)	(3,0)	(3,1)
$K_{\langle x,y\rangle}$	7.529	2.496	4.378
$\tilde{K}_{\langle x,y\rangle}$	7.526	2.497	4.387
Error	−0.03%	−0.16%	0.07%

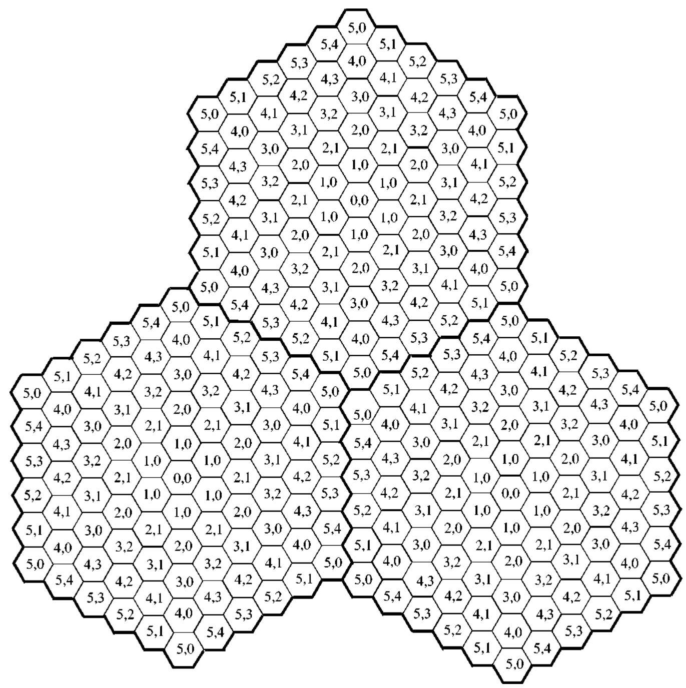

Fig. 9. Type assignment of microcells in three neighboring macrocells.

VI. Applications for the New Random Walk Model

This section describes three applications that can utilize our random walk model: microcell/macrocell PCS network modeling, distance-based location update modeling, and *General Packet Radio Service* (GPRS) mobility management modeling.

In a microcell/macrocell PCS network [4], [11], [20], the service area is covered by both microcell BS's and the macrocell BS's. A macrocell overlays several microcells to increase the circuit capacity. An example of the microcell/macrocell configuration is the dual-band GSM network deployed by Far EasTone in Taiwan [15]. In this network, there are two types of *base transceiver stations* (BTS's). The DCS 1800 BTS's serve for microcells, which operate at 1.8 GHz. The GSM 900 BTS's serve for macrocells, which operate at 900 MHz. The typical coverage area of a microcell is between 0.5 and 3 km, and the area of a macrocell is between 3 and 10 km. In modeling microcell/macrocell configuration, it is required to derive the MS residence time distribution at a macrocell based on the MS residence time distribution at the microcells. Our new random walk model can be used for the derivation of the macrocell residence time distribution. The first step is to classify the types of microcells within a macrocell. Fig. 9 plots three neighboring macrocells and type assignment of microcells in these macrocells. For a specific type of microcell, we use (2) to compute the number of microcells that are visited before the MS moves out of the macrocell. The residence times of these microcells are accumulated to derive the time before the MS leaves the macrocell. The modeling details can be found in [15].

Another application of the new random walk is the modeling of *distance-based* location update scheme. In existing PCS networks, the service area is partitioned into several *location areas* (LA's). Each LA consists of a group of cells and each MS performs a location update whenever it enters an LA [6], [14]. The location information is stored in the location databases such as home location register and visitor location register. When an incoming call arrives, the network retrieves the location databases to identify the LA where the MS resides. All cells in the LA are paged to find the MS for call delivery. In [3], three location update schemes were proposed. In the *time-based* scheme, after a location update, a timer is set for the MS. When the timer expires, the MS performs the next location update. In the *movement-based* scheme, after a location update, a counter is set for the MS. When the MS moves across a cell boundary, the counter is incremented by one. When the counter value reaches a threshold, the MS performs the next location update. In the *distance-based* scheme, when the distance between the cell where the previous location update was made and the current cell is longer than a threshold, the next location update is performed. Results demonstrated that distance-based scheme has the best performance [10], [1]. In [2], analytical models were proposed to study the costs of paging and location updates for the distance-based scheme. A simple random walk was used to investigate the MS movement, which introduces inaccuracy. With the new random walk proposed in this paper, accurate user moving behavior can be modeled.

A third application of the new random walk is the modeling of *General Packet Radio Service* (GPRS) mobility management. GPRS [7] provides data services for digital TDMA systems such as GSM [13], [16], [17] or Digital AMPS (IS-136) [12], [5]. To support GPRS, a new data protocol called *GPRS Tunneling Protocol* (GTP) [8] is developed to route the GPRS packet data to the external data networks. To accurately route data using GTP, traditional GSM mobility management [6] is modified. Besides LA's, GPRS tracks the *routing area* (RA) of a GPRS MS. An RA is a group of cells, which is a subset of an LA. When a GPRS MS moves to a new RA, an RA update is performed. When the MS moves to a new LA, separate RA and LA updates or a combined RA/LA update is required. It is clear that LA/RA updates are more expensive than pure RA updates. Thus, it is desirable to configure an appropriate LA/RA layout based on the MS data/call traffic. Our random walk model can be used to determine the number of RA's visited before the MS moves to the new LA. This piece of information is then used in GPRS LA/RA modeling to determine LA/RA layout.

VII. Conclusion

This paper proposed a new approach to simplify the two-dimensional random walk models capturing the movement of mobile users in PCS networks. Analytical models were proposed for the new random walks with both hexagonal and mesh configurations. Our method significantly reduces the states in the random walks and thus, the execution times to derive the output measures. Specifically, for the hexagonal configuration, we reduce the number of states from $(2n^2-2n+1)$ to $n(n+1)/2$. For the mesh configuration, the number is reduced from $(3n^2+3n-5)$ to $(n^2+2n+4)/4$ if n is even and to $(n^2+2n+5)/4$ if n is odd. Simulation experiments were conducted to validate the analytical models. The results indicated that the errors between the analytical and simulation models are within 1%.

References

[1] I. F. Akyildiz and J. S. M. Ho, "Dynamic mobile user location update for wireless PCS networks," *ACM-Baltzer J. Wireless Networks*, vol. 1, no. 1, pp. 187–196, 1995.

[2] I. F. Akyildiz, J. S. M. Ho, and Y.-B. Lin, "Movement-based location update and selective paging for PCS network," *IEEE/ACM Trans. Networking*, vol. 4, no. 4, pp. 629–638, Aug. 1996.

[3] A. Bar-Noy, I. Kessler, and M. Sidi, "Mobile users: To update or not to update?," *ACM/Baltzer Wireless Networks*, vol. 1, no. 2, pp. 187–196, 1994.

[4] R. Beraldi, S. Marano, and C. Mastroianni, "Performance of a reversible hierarchical cellular system," *Int. J. Wireless Inform. Networks*, vol. 4, no. 1, pp. 43–54, 1997.

[5] EIA/TIA, "800 MHz TDMA cellular-radio interface-mobile station-base station compatability-digital control channel," EIA/TIA, Tech. Rep. IS-136, 1994.

[6] ETSI/TC, "Mobile application part (MAP) specification, version 4.8.0," ETSI, Tech. Rep. Recommendation GSM 09.02, 1994.

[7] ——, "GPRS service description stage 2," ETSI, Tech. Rep. Recommendation GSM GSM 03.60 Version 7.0.0 (Phase 2+), 1998.

[8] ——, "GPRS tunnelling protocol (GPT) across the Gn and Gp interface," ETSI, Tech. Rep. Recommendation GSM GSM 09.60 version 7.0.0 (Phase 2+), 1998.

[9] W. Feller, *An Introduction to Probability Theory and Its Applications, Volume I*. New York: Wiley, 1966.

[10] J. S. M. Ho and I. F. Akyildiz, "Mobile user location update and paging under delay constraints," *ACM-Baltzer J. Wireless Networks*, vol. 1, no. 4, pp. 413–426, 1995.

[11] C.-L. I, L. J. Greenstein, and R. D. Gitlin, "A microcell/macrocell cellular architecutre for low- and high-mobility wireless users," *IEEE J. Select. Areas Commun.*, vol. 11, pp. 885–891, 1993.

[12] W. C. Y. Lee, *Mobile Cellular Telecommunications Systems*. New York: McGraw-Hill, 1995.

[13] Y.-B. Lin, "No wires attached: Reaching out with GSM," *IEEE Potentials*, Oct./Nov. 1995.

[14] ——, "Mobility management for cellular telephony networks," *IEEE Parallel Distributed Technol.*, vol. 4, pp. 65–73, Nov. 1996.

[15] Y.-B. Lin, W. R. Lai, and R. J. Chen, "Performance analysis for dual band PCS networks," *IEEE Trans. Computers*, 2000.

[16] M. Mouly and M.-B. Pautet, *The GSM System for Mobile Communications* Palaseau, France, 1992.

[17] S. Redl and M. Weber, *An Introduction to GSM*. Norwood, MA: Artech House, 1995.

[18] S. M. Ross, *Stochastic Processes*. New York: Wiley, 1983.

[19] ——, *Introduction to Probability Models*. New York: Academic, 1985.

[20] L.-C. Wang, G. L. Stüber, and C.-T. Lea, "Architecture design, frequency planning, and performance analysis for a microcell/macrocell overlaying system," *IEEE Trans. Veh. Technol.*, vol. 46, pp. 836–848, 1997.

Ian F. Akyildiz (F'95) is a Professor with the School of Electrical and Computer Engineering, Georgia Institute of Technology and Director of Broadband and Wireless Networking Laboratory. His current research interests are in Wireless Networks, Satellite Communication, ATM Networks, Next Generation Internet.

Dr. Akyildiz is an ACM Fellow. He received the Don Federico Santa Maria Medal for his services to the Universidad of Federico Santa Maria in Chile. He served as a National Lecturer for ACM from 1989 until 1998 and received the ACM Outstanding Distinguished Lecturer Award for 1994. He is the Editor-in-chief of *Computer Networks* (Elsevier). He received the 1997 IEEE Leonard G. Abraham Prize award for his paper entitled "Multimedia Group Synchronization Protocols for Integrated Services Architectures" published in the IEEE Journal of Selected Areas in Communications (JSAC) in January 1996. He was the program chair of the 9th IEEE Computer Communications workshop, and served as the program chair for ACM/IEEE MOBICOM'96 (Mobile Computing and Networking) conference as well as for IEEE INFOCOM'98 conference.

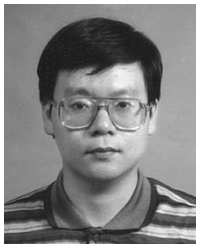

Yi-Bing Lin (S'80–M'96–SM'96) received the B.S.E.E. degree from National Cheng Kung University in 1983, and the Ph.D. degree in computer science from the University of Washington in 1990.

From 1990 to 1995, he was with the Applied Research Area at Bell Communications Research (Bellcore), Morristown, NJ. In 1995, he was appointed as a Professor of Department of Computer Science and Information Engineering (CSIE), National Chiao Tung University (NCTU). In 1996, he was appointed as Deputy Director of Microelectronics and Information Systems Research Center, NCTU. During 1997–1999, he was elected as Chairman of CSIE, NCTU. His current research interests include design and analysis of personal communications services network, mobile computing, distributed simulation, and performance modeling.

Dr. Lin is an Associate Editor of IEEE NETWORK, an Editor of IEEE J-SAC: Wireless Series, an Editor of IEEE PERSONAL COMMUNICATIONS MAGAZINE, a Guest Editor for IEEE TRANSACTIONS ON COMPUTERS special issue on Mobile Computing, and a Guest Editor for IEEE COMMUNICATIONS MAGAZINE special issue on Active, Programmable, and Mobile Code Networking. He received the 1997 Outstanding Research Award from National Science Council, ROC, and Outstanding Youth Electrical Engineer Award from CIEE, ROC.

Wei-Ru Lai received the B.S.E.E and Ph.D. degrees from the Department of Computer Science and Information Engineering, National Chiao Tung University in 1991 and 1999, respectively.

In 1999, she was appointed as an Assistant Professor and was elected as Chairman of Department of Information Management, Chin-Min College. Her current research interests include design and analysis of personal communications services network.

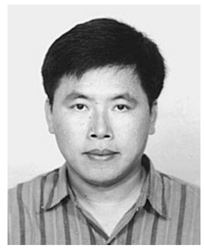

Rong-Jaye Chen was born in Taiwan in 1952. He received the B.S. degree in mathematics from National Tsing Hua University in 1977, and the Ph.D. degree in computer science from the University of Wisconsin-Madison in 1987.

He is currently a Professor and Chairman of Computer Science and Information Engineering Department in National Chiao Tung University. His research interests include cryptography and security, personal communication service, algorithm design, and theory of computation.